Scilight

Journal of Mechanical Engineering and Manufacturing
https://www.sciltp.com/journals/jmem



Review

Check for updates

The Relationship between Tool Coatings and Process Parameters on Cutting Forces and Wear in High-Speed Machining

Naiara P. V. Sebbe [1,2,*], Andresa Baptista [1,3], Gustavo Pinto [1,3], Rúben D. Costa [2], Wenfeng Ding [4], Rafaela Barros Casais [1] and Rita Sales-Contini [5]

[1] CIDEM, ISEP, Polytechnic of Porto, Rua Dr. António Bernardino de Almeida, 4249-015 Porto, Portugal
[2] FEUP—Faculty of Engineering, University of Porto, 4200-465 Porto, Portugal
[3] LAETA-INEGI, Associate Laboratory for Energy, Transports and Aerospace, Rua Dr. Roberto Frias 400, 4200-465 Porto, Portugal
[4] College of Mechanical and Electrical Engineering, Nanjing University of Aeronautics and Astronautics, Nanjing 210016, China
[5] Aeronautical Structures Laboratory, Technological College of São José dos Campos Prof. Jessen Vidal (FATEC), São José dos Campos, São Paulo 12247-014, Brazil
* Correspondence: napvs@isep.ipp.pt (N.P.V.S.); Tel.: +351-22-83-40-500

How To Cite: Sebbe, N.P.V.; Baptista, A.; Pinto, G.; et al. The Relationship between Tool Coatings and Process Parameters on Cutting Forces and Wear in High-Speed Machining. *Journal of Mechanical Engineering and Manufacturing* **2026**. https://doi.org/10.53941/jmem.2026.100036

Received: 31 March 2026
Revised: 9 May 2026
Accepted: 12 August 2026
Published: 15 October 2026

Abstract: This paper provides a comprehensive analysis of cutting force dynamics in High-Speed Machining (HSM), a critical factor for ensuring structural integrity and productivity in advanced manufacturing. The study synthesizes the role of piezoelectric dynamometry and the Finite Element Method (FEM) in predicting and monitoring force vectors during the processing of difficult-to-cut alloys, specifically Inconel 718 and Ti–6Al–4V. A critical investigation is conducted into how tool edge micro-geometry and nanostructured coatings (e.g., AlTiN, ZrN) manipulate the thermomechanical interface, leveraging the thermal softening effect to counteract high work-hardening rates. Furthermore, the research evaluates the impact of lubrication strategies, such as Minimum Quantity Cooling Lubrication (MQCL), and tool-path kinematics, including ramp, helical, and plunge entries, on the stability of cutting forces and sub-surface integrity. To bridge the gap between laboratory findings and industrial scalability, a strengths, weaknesses, opportunities, and threats (SWOT) analysis is employed, identifying the strengths of adiabatic shearing and the threats of dynamic instability. The findings conclude that the synergy between precise parameter selection and real-time force feedback is essential for mitigating the "size effect" and preventing catastrophic tool failure. This review serves as a technological roadmap for implementing data-driven HSM processes, emphasizing the transition toward sustainable, zero-defect manufacturing in the aerospace and mold-making sectors. Unlike previous reviews that focus solely on material properties, this study establishes a novel integrated framework that correlates tool coating synergistic effects with dynamic process parameters specifically for difficult-to-cut alloys. The scientific novelty lies in the systematic identification of the 'coating-parameter-wear' nexus, providing a predictive perspective for optimizing high-speed machining through a combined SWOT-FEM analytical approach.

Keywords: high-speed machining (HSM); cutting force dynamics; nanostructured tool coatings; machinability of superalloys; finite element method (FEM); piezoelectric dynamometry; surface integrity

Copyright: © 2026 by the authors. This is an open access article under the terms and conditions of the Creative Commons Attribution (CC BY) license (https://creativecommons.org/licenses/by/4.0/).
Publisher's Note: Scilight stays neutral with regard to jurisdictional claims in published maps and institutional affiliations.

1. Introduction

High-Speed Machining (HSM) has emerged as a pivotal technology in modern manufacturing, characterized not only by elevated spindle speeds but primarily by a significant increase in Material Removal Rate (MRR) [1]. This process is fundamental for industries demanding high precision and superior surface integrity, such as aerospace and mold-making [2]. Theoretically, HSM operates in a regime where increasing cutting speeds leads to a reduction in cutting forces due to the thermal softening of the workpiece material, which facilitates plastic deformation [3].

The integration of HSM in the aerospace sector faces significant hurdles when machining difficult-to-cut materials, such as titanium and nickel-based alloys. As emphasized by Zhao et al. [4], these materials often lead to rapid tool degradation and poor surface integrity due to extreme mechanical loads. To mitigate these effects, the adoption of hybrid processes, where traditional HSM is assisted by external energies like laser, ultrasonic vibrations, or advanced cooling, has proven essential, as these methods locally modify material response to reduce resultant cutting forces. This challenge is further detailed by Raghavendra et al. [5] in their study of the Ti–6Al–4V (titanium alloy), where heat generated by the material's low thermal conductivity causes approximately 80% of the generated heat to dissipate directly into the tool. Consequently, their research demonstrates that beyond hybrid assistance, the precise optimization of machining parameters, such as coolant flow rate, cutting speed, and the use of PVD (physical vapour deposition)-coated inserts, is critical to managing tool wear and ensuring process stability in high-speed regimes.

Building upon this, the transition to high-speed regimes introduces complex thermo-mechanical challenges where the selection of cutting tools becomes a decisive factor [6]. These tools must possess superior hot-hardness and chemical stability to withstand the intense thermal gradients and cyclic loads inherent to the process [7]. Recent advancements emphasize that tool performance is heavily dictated by thin-film coatings (e.g., TiAlN, AlTiN, or diamond-like carbon (DLC)), which function as both thermal barriers and solid lubricants to reduce the friction coefficient at the tool-chip interface [8,9].

The evolution of tool performance in HSM is intrinsically linked to the advancement of thin-film architecture. As reviewed by Dabees et al. [10], the strategic application of physical vapour deposition (PVD) and chemical vapour deposition (CVD) coatings, ranging from nitrides to borides, creates a thermal and chemical barrier that prevents direct contact between the workpiece and the tool substrate, fundamentally altering the temperature distribution in the cutting zone. This structural benefit is further enhanced using multilayered nano-coatings; according to Ganeshkumar et al. [11], materials such as TiAlN and CrAlSiN not only provide superior hardness (reaching up to 32 GPa) but also significantly reduce vibration emissions and cutting forces. However, managing these variables in real-time remains a challenge, leading to the development of data-driven solutions. In this context, Guo et al. [12] proposed an interpretable deep learning approach using a multi-scale pyramid attention network (MPAN) to monitor tool wear. By introducing prior knowledge of signal periodicity into the network design, their method allows for the accurate extraction of features from sensory signals, bridging the gap between complex black-box artificial intelligence (AI) models and the physical reality of high-speed milling. Together, these studies emphasize that the future of HSM lies in the synergy between advanced material science and interpretable monitoring technologies to ensure process stability and cost-efficiency.

Regarding "autonomous tuning", the reviewed literature indicates two complementary AI directions with different maturity levels: (i) signal-based tool-condition monitoring, where convolutional neural networks (CNNs) and attention-based temporal models (e.g., Transformer-style blocks) learn wear-sensitive features from dynamometry/AE/vibration signals (as exemplified by the MPAN approach in [12]); and (ii) decision-making for parameter/path adaptation, where Reinforcement Learning (RL) is increasingly explored to optimize tool-path or process parameters under constraints (force limits, surface integrity, and tool-wear rate), using either data-driven surrogates or simplified physics models as the environment. A practical roadmap is therefore hybrid: deploy CNN/attention models first for reliable state estimation (wear and force anomalies), then close the loop via constrained RL or model-predictive control to adjust feed/speed and path segments without violating stability limits.

In the machining of difficult-to-cut materials, such as Titanium (Ti) and Nickel (Ni) superalloys, the operational process window is remarkably narrow due to their low thermal conductivity and high thermo-chemical affinity with cutting tool materials [13–22]. These alloys are inherently prone to rapid tool degradation through complex mechanisms of adhesion, attrition, and diffusion [23,24]. While intensifying coolant pressure or employing cryogenic assistance can mitigate heat accumulation and facilitate chip segmentation, transitioning from continuous to serrated or segmented morphologies, such interventions introduce stochastic variables into the force dynamics [25]. Consequently, the precise quantification of cutting forces in these high-strain-rate regimes is

no longer merely a diagnostic exercise; it has become a fundamental requirement for multi-objective process optimization and the prevention of catastrophic tool failure [26].

Despite the established maturity of experimental methods, such as high-frequency piezoelectric dynamometry, and the predictive capabilities of Finite Element Method (FEM) modeling using constitutive equations like Johnson-Cook (J-C), a critical gap remains in the literature regarding the seamless integration of these domains. There is an urgent need to synthesize how empirical sensor data and numerical simulations can be synergistically combined to enable real-time force control and adaptive machining strategies. This review aims to systematically analyze current methodologies for the measurement, prediction, and active control of cutting forces in HSM. By evaluating the latest advancements in sensor fusion and computational efficiency, this paper identifies the most effective strategies to enhance tool life, ensure surface integrity, and maintain production stability in the era of intelligent manufacturing.

2. Methodology

To ensure a robust and systematic analysis of cutting force dynamics in High-Speed Machining (HSM), this study follows a multi-step methodological framework. The review process was designed to synthesize findings from core peer-reviewed articles, ensuring both breadth in experimental data and technical depth in numerical modeling.

2.1. Literature Selection and Data Acquisition

The research was conducted across major scientific databases (e.g., ScienceDirect, SpringerLink, and Scopus), focusing on peer-reviewed articles primarily published in the last decade to capture recent advancements. The selection criteria prioritized:

- Process regimes: studies focusing on high-speed ranges where adiabatic shearing and thermal softening effects significantly alter the conventional chip formation mechanism;
- Material focus: investigations involving difficult-to-cut alloys, specifically Titanium (Ti–6Al–4V (titanium alloy)) and Nickel-based superalloys (Inconel 718), due to their critical role in aerospace applications;
- Analysis methods: articles providing quantitative data from piezoelectric dynamometry, Finite Element Method (FEM) simulations, and tool wear characterization.

Inclusion criteria: studies were selected based on (1) explicit reporting of cutting force components; (2) use of advanced tool materials or coatings (physical vapour deposition (PVD)/chemical vapour deposition (CVD)); and (3) validation of numerical models through experimental data.

Exclusion criteria: studies lacking clear machining parameters (speed, feed, depth of cut), grey literature, and articles focusing solely on low-speed conventional machining were excluded.

2.2. Comparative Parameters and Interfacial Analysis

Data extraction followed a standardized protocol where findings were categorized into three analytical pillars to allow for a comparative synthesis:

(1) Experimental dynamometry: analysis of signal acquisition, frequency response, and the impact of tool-workpiece engagement on force oscillations;
(2) Numerical and predictive modeling: evaluation of constitutive laws (e.g., Johnson-Cook) and the accuracy of FEM in predicting stress and thermal gradients;
(3) Tribological and surface integrity: correlation between force dynamics, tool coating performance, and the resulting surface roughness and residual stresses.

2.3. Optimization and Technological Readiness Framework

To bridge the gap between laboratory research and industrial scalability, a critical evaluation was performed based on:

- Technical performance: precision of force prediction and effectiveness of real-time monitoring systems (e.g., Deep Learning approaches);
- Economic feasibility: relationship between cutting force reduction and tool life extension, analyzed through the lens of a SWOT framework to evaluate industrial implementation;
- Innovation potential: compatibility with Industry 4.0 standards, including sensor fusion and adaptive control strategies.

3. State-of-the-Art in High-Speed Machining Force Dynamics and Monitoring

3.1. Fundamentals and Methodologies for Cutting Force Quantification

Precise knowledge of cutting forces is a fundamental prerequisite for estimating cutting temperatures, predicting tool life, and performing chatter analysis [27,28]. The mechanics of machining and the prediction of these forces have been extensively modeled, as understanding these dynamics allows for the mitigation of processing issues such as vibrations, tool overloads, and premature failure [29]. Furthermore, the selection of tool coatings and the optimization of microgeometry, including honed or chamfered edges, are critical, as they directly influence the friction coefficient, the surface finish of the machined part, and the overall tool service life [30].

In the context of High-Speed Machining (HSM), the pursuit of higher material removal rates (MRR) and improved machinability has led research to focus on three main pillars: advanced tool materials, efficient lubrication/cooling strategies, and thermally enhanced processes (e.g., laser or plasma-assisted machining) [31]. To optimize these variables, real-time monitoring via sensors, such as dynamometers, accelerometers, and acoustic emission (AE) sensors, has become essential. The signals acquired from these devices enable a data-driven approach to parameter adjustment and defect reduction [32].

Currently, cutting forces are determined through a dual approach involving empirical/analytical models and numerical methods, such as the Finite Element Method (FEM) [33]. Experimentally, while forces can be estimated via the current consumption of spindle motors, high-precision quantification is typically achieved using piezoelectric, capacitive, or strain-gauge dynamometers [34]. These systems track physical parameter changes during the cutting process, providing the necessary data to validate predictive models and ensure process stability [35].

3.2. Predictive Modeling: The Role of Finite Element Method (FEM) in HSM

The Finite Element Method (FEM) has established itself as an indispensable tool for characterizing the thermo-mechanical phenomena that are otherwise inaccessible through experimental means [36]. Beyond predicting cutting and feed forces, FEM allows for the granular analysis of plastic strain rates, localized stresses, and the intricate morphology of chip formation [37].

The predictive accuracy of FEM in HSM is fundamentally dependent on the robustness of the constitutive models employed, such as the Johnson-Cook (J-C) law, which accounts for the combined effects of strain hardening, strain-rate sensitivity, and thermal softening. In high-speed regimes, where strain rates can exceed 10^5 s^{-1} and temperatures at the tool-chip interface often surpass 1000 °C, the numerical integration of these variables is critical for replicating the adiabatic shear banding that leads to serrated chip formation. Furthermore, advanced Arbitrary Lagrangian–Eulerian (ALE) formulations have mitigated the traditional mesh distortion issues associated with large plastic deformations, allowing for a more stable and continuous simulation of the tool's engagement with the workpiece material, thereby providing a more precise estimation of the cyclic force oscillations.

Beyond the immediate calculation of force vectors, FEM serves as a virtual laboratory for engineering the surface integrity of critical components. By simulating the unloading phase and subsequent cooling of the workpiece, numerical models can predict the distribution of residual stresses, both compressive and tensile, which are decisive factors for the fatigue life of aerospace parts. This capability enables researchers to perform sensitivity analyses on edge micro-geometries and coating thicknesses before physical prototyping, significantly reducing the cost and time-to-market for specialized tooling. Consequently, the integration of FEM into the design cycle represents a shift from reactive trial-and-error methodologies to a proactive, physics-based optimization of the HSM process.

3.2.1. Computational Formulations: Eulerian vs. Lagrangian

In the numerical modeling of HSM, the choice of the computational framework is dictated by the nature of the deformation [38,39].

- Lagrangian analysis [40]: the computational grid deforms alongside the material. While excellent for tracking free surfaces and complex tool geometries, it often requires frequent remeshing to handle the extreme distortions typical of high-speed shearing.
- Eulerian analysis [41]: the mesh remains fixed in space as the material flows through it. This is mathematically efficient for steady-state cutting but less effective for capturing transient chip initiation.

For the highly non-linear and dynamic nature of HSM, explicit time integration is generally preferred over implicit techniques, as it better captures the high-frequency response of the tool-workpiece interaction [42,43]. To overcome the individual limitations of these frameworks, the Arbitrary Lagrangian-Eulerian (ALE) formulation has emerged as the most robust approach for HSM simulations [44]. By combining the strengths of both methods,

ALE allows the mesh to move independently of the material flow, effectively preventing the severe element distortion that causes premature termination in pure Lagrangian models. This flexibility is particularly critical when simulating the high-temperature gradients at the tool-chip interface, as it maintains a high-quality mesh in the secondary shear zone, ensuring that the predicted friction-induced heat and the resulting cutting forces remain numerically stable throughout the steady-state phase.

Furthermore, the selection between these formulations directly impacts the accuracy of the predicted residual stresses and the thermal distribution within the workpiece. While Eulerian models provide rapid convergence for continuous chip formation, they often struggle to accurately represent the 'chip root', the critical area where the material separation occurs. Conversely, Lagrangian models, when coupled with advanced adaptive remeshing techniques, excel at capturing the localized adiabatic shear bands that lead to serrated chips. Therefore, the contemporary shift in predictive modeling favors an integrated approach, where the explicit time integration of ALE-based solvers is calibrated against high-frequency experimental data to ensure that the virtual environment faithfully replicates the high-strain-rate physics of advanced alloy machining [45–47].

3.2.2. Critical Attributes for Robust Simulation

To ensure that a FEM model reflects physical reality, three analytical pillars must be addressed [48–50]:

(1) Constitutive modeling: the material model (typically the Johnson-Cook law) must accurately represent the coupled effects of strain hardening, strain-rate sensitivity, and thermal softening.
(2) Chip separation mechanisms: advanced models now favor Adaptive Meshing or damage-based criteria over simplistic geometric separation, particularly when analyzing the influence of tool edge micro-geometry (honed or chamfered edges).
(3) Interfacial friction: modeling the tool-chip contact requires sophisticated friction laws (e.g., modified Coulomb or Zorev models) to account for the secondary shear zone's heat generation.

Despite the theoretical maturity of these three pillars, their practical implementation in HSM simulations remains a significant challenge due to the high degree of interdependence between them. For instance, the Constitutive Modeling of advanced alloys like Inconel 718 or Ti–6Al–4V often relies on Johnson-Cook parameters derived from Split-Hopkinson pressure bar (SHPB) tests. However, these tests rarely reach the extreme strain rates and localized temperatures found in the primary shear zone of HSM, leading to a 'calibration gap' that can result in a 20–30% error in predicted cutting forces if not meticulously tuned against experimental benchmarks.

Furthermore, the Chip Separation and Interfacial Friction mechanisms are often oversimplified as static constants. In fact, the friction coefficient at the tool-chip interface is a dynamic function of the local pressure and temperature, which are dictated by the tool's micro-geometry and the chip morphology. A critical limitation in current literature is the 'black box' approach to the secondary shear zone; while Zorev's model accounts for sticking and sliding zones, it frequently fails to incorporate the tribological influence of nanostructured coatings or the penetration of MQCL mists. Therefore, for a simulation to be truly robust, it must transition from deterministic models to adaptive, multi-physics frameworks that can recalibrate these interfacial parameters in real-time as the tool engages with the workpiece.

3.2.3. From 2D Orthogonal to 3D Comprehensive Models

While 2D orthogonal simulations provide valuable insights into the primary shear zone and temperature gradients, highlighting the adiabatic shearing effect where heat is localized within the chip, they remain a simplification. As shown in studies using specialized software like DEFORM-3D, transitioning to 3D simulations is mandatory for capturing the true volumetric force distribution. This transition allows for the inclusion of the actual tool nose radius, feed-rate effects, and the complex 3D flow of the chip, which are essential for precise force quantification in industrial HSM applications [51].

The shift to 3D comprehensive modeling is particularly critical when analyzing the influence of the tool's lead angle and inclination angle on the resultant force vector. Unlike 2D orthogonal cutting, which assumes a constant width of cut, 3D simulations capture the varying chip thickness across the tool nose radius, a region where the 'size effect' is non-uniform and the effective rake angle changes continuously along the cutting edge. This spatial complexity is the primary driver of the axial and radial force components, which are responsible for tool deflection and surface dimensional errors. By incorporating the full tool geometry and the 3D helical motion of the tool path, researchers can predict not only the magnitude of the forces but also their directionality, which is vital for optimizing the stiffness of the machine-tool-workpiece system.

Furthermore, 3D modeling facilitates the study of complex chip-evacuation dynamics and their impact on secondary force fluctuations. In high-speed milling, the centrifugal forces acting on the chip and the interaction

with the tool's flutes create a transient loading environment that 2D models inherently ignore. Advanced 3D FEM frameworks now allow for the simulation of multi-step machining sequences, where the residual stress and thermal state from a previous pass are carried over to the next. This 'digital twin' approach to the machining process enables the prediction of part distortion in thin-walled aerospace components, moving beyond simple force estimation toward a holistic assessment of the manufacturing chain's stability and precision.

3.3. Experimental Characterization of Cutting Forces

The experimental quantification of cutting forces remains the "gold standard" for validating numerical models, as illustrated in Figure 1, which shows a typical setup in a hard machining center, and understanding the stochastic nature of the machining process. As highlighted in the literature, predicting these forces is inherently complex due to the interplay of tool deflection, machine tool dynamics, and workpiece material behavior [52]. Beyond mere diagnostic data, the monitoring of cutting forces is of paramount importance for the global optimization of machining cycles, providing critical insights into the fundamental cutting behavior of specialized tooling. Furthermore, as emphasized by real-time force determination is a primary driver for the evolution of cutting-tool technology; it enables the systematic evaluation of novel coating architectures and innovative micro-geometries, directly revealing how these advancements influence the mechanics of force generation and thermal dissipation at the tool-chip interface [53].

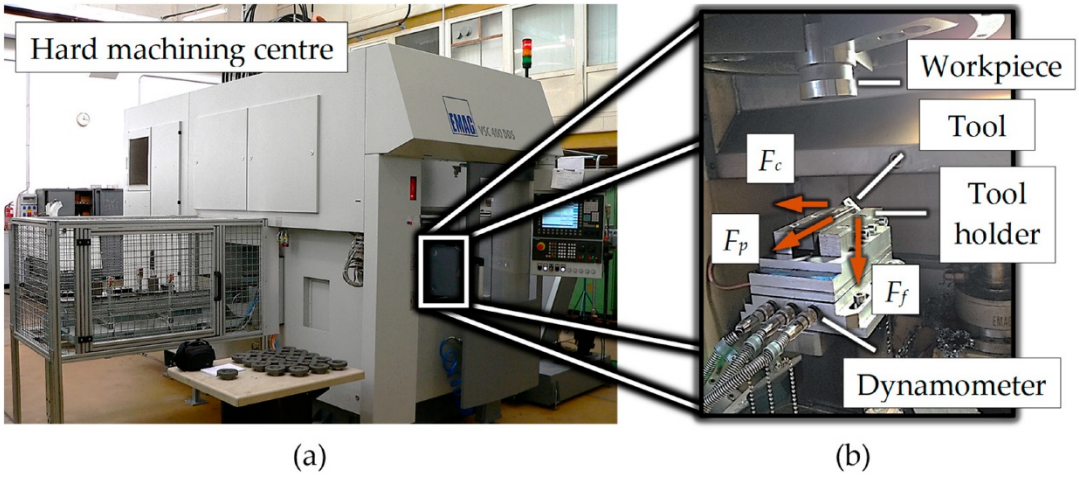


Figure 1. Experimental characterization of cutting forces in a production environment: (**a**) Overview of the hard machining center, and (**b**) Detailed view of the piezoelectric dynamometer setup for decomposing the resultant force into tangential (cutting force, F_c), axial (axial force, F_p), and feed (feed force, F_f) components during tool-workpiece interaction. Reproduced from [54].

3.3.1. Instrumentation and Advanced Sensing

The determination of cutting forces in HSM can be approached through various experimental techniques, ranging from indirect power consumption analysis to high-fidelity direct sensing. Traditionally, the current consumption of the machine tool's driving motors has been used as an indicator of machining load; however, this method often lacks the sensitivity required to capture rapid force transients and high-frequency oscillations. Consequently, modern experimental setups rely on specialized force-sensing systems, such as piezoelectric, capacitive, optoelectrical, and strain-gauge dynamometers. These instruments track specific physical changes, such as micro-displacements or electrical charges, induced by the cutting force, enabling real-time monitoring and post-process data analysis for structural optimization [55].

From a signal-quality perspective, high-frequency HSM imposes substantially harsher signal-to-noise ratio (SNR) constraints than low-speed conventional machining: force and vibration content shifts toward higher frequencies (tooth-passing harmonics, impacts, and chatter sidebands), while electromagnetic interference and structural resonances increase the noise floor. Piezoelectric dynamometers are generally preferred for HSM because of their high stiffness and wide bandwidth, enabling capture of fast transients, but they are sensitive to mounting/preload and can exhibit drift that must be compensated in long runs. Capacitive/optoelectrical approaches can achieve high resolution for micro-displacements, yet their practical SNR can degrade in production due to thermal expansion, coolant mist contamination, and the need for stable gap control. Strain-gauge platforms are robust and cost-effective, but their lower natural frequencies and higher susceptibility to structural compliance

can attenuate high-frequency content, making them more suitable for low-speed operations or quasi-static force monitoring unless carefully designed for high bandwidth.

In the study conducted by Daniyan et al. [56], Response Surface Methodology (RSM) was successfully employed to correlate process parameters with empirical data obtained from a Kistler piezoelectric dynamometer. This dual approach allows for the identification of optimal machining windows by comparing actual values with predicted statistical models. The result of this experiment is illustrated in Figure 2. Furthermore, ultra-precision machining studies, such as those by Brinksmeier et al. [51], utilize sophisticated setups where the tool is mounted on high-sensitivity force transducers (e.g., Kistler 9256C1) within air-bearing spindle systems. These configurations are essential for face turning experiments, providing a continuous function of cutting forces relative to varying cutting speeds. However, moving from laboratory settings to industrial environments requires more flexible and cost-effective solutions. In this context, Wan et al. [57] proposed an industry-oriented method to indirectly measure cutting forces by monitoring the deflections of the rotating tool shank using displacement sensors. By applying substructure synthesis to determine tool stiffness, rather than relying on traditional inverse calibration, their approach eliminates the need for a reference dynamometer in situ. Validated against Kistler 9255B, this method demonstrates that tracking the gap variations between the sensor and the tool shank provides a reliable and 'friendly' alternative for real-time force monitoring in high-speed milling operations, bridging the gap between high-end research instrumentation and practical shop-floor applications.

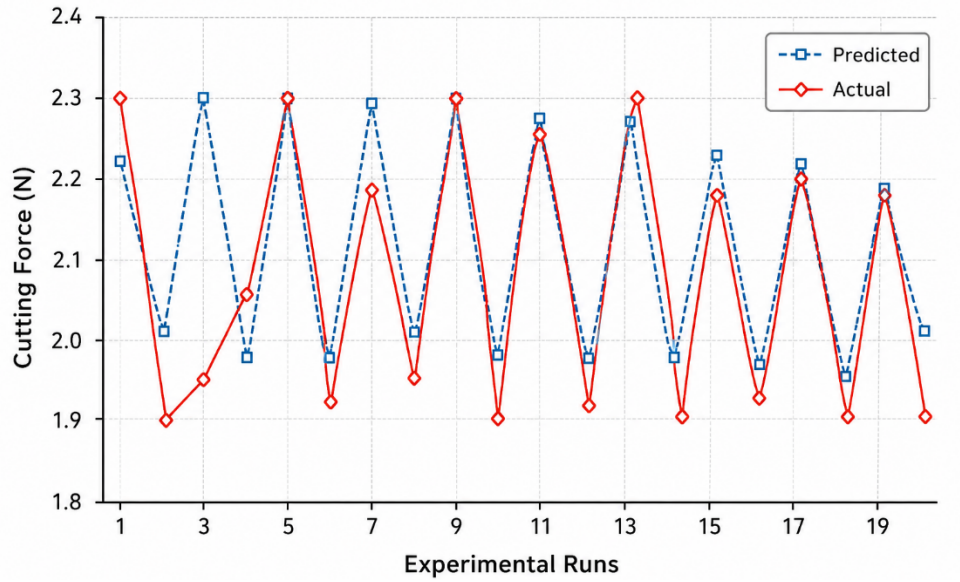


Figure 2. Scatter plot comparing the experimentally measured cutting forces (Actual) with the values predicted by the Response Surface Methodology (RSM) across different experimental runs. Reproduced from [56].

3.3.2. Force Dynamics and Tool Material Influence

The choice of tool material, whether Single Crystal Diamond (SCD), Polycrystalline Diamond (PCD), or Carbide, significantly alters the force signatures due to differences in thermal conductivity and mechanical properties [58]. Key observations from the state-of-the-art include:

- Repeatability and directionality: high-fidelity measurements in materials like brass (CuZn39Pb3) and aluminum (AlMg5) demonstrate excellent repeatability. Even when the feed direction is reversed, the force profiles remain consistent, validating the stability of the experimental sensing systems [51].
- The transition point "A": a critical phenomenon observed in HSM is the transition to adiabatic shearing (indicated as point "A" in force diagrams). At this juncture, the localized heat generation causes a shift in the material's flow stress, directly impacting the cutting (cutting force, F_c), normal (normal force, F_n), and feed (feed force, F_f) forces.
- Force inversion: in specific materials like AlMg5 turned with SCD tools, a distinctive behavior occurs where the thrust force exceeds the cutting force beyond a critical speed, signaling a change in the tool-chip contact mechanics.

The phenomena described, particularly the 'Transition Point A' and 'Force Inversion', reveal a fundamental shift in the energy balance of the high-speed cutting zone. The transition to adiabatic shearing at point 'A' is best interpreted as a thermo-mechanical system threshold where the rate of heat generation through plastic deformation outpaces the ability of the coupled tool–chip–workpiece system to dissipate that energy. Consequently, 'Point A'

should not be treated as a fixed intrinsic material constant: while alloy-dependent features (thermal conductivity, strain-rate sensitivity and work-hardening) influence when localization becomes energetically favorable, the observed transition is strongly modulated by system-dependent variables that control heat partitioning and interface friction. In practice, tool thermal diffusivity (and its alteration by coatings), edge micro-geometry, contact length, and cooling/lubrication strategy can shift the onset of localization by acting as heat sinks/insulators and by changing the sticking–sliding balance at the rake face. When SCD tools are employed, their extreme thermal conductivity (>2000 W/m·K) acts as a heat sink, potentially delaying this adiabatic transition compared to Carbide tools. Therefore, a more transferable way to report Point A is to relate it to the governing heat-partition/thermal time-scale balance (and the associated force-vector change), rather than to cutting speed alone.

Furthermore, the observation of 'Force Inversion' (where thrust force exceeds cutting force) challenges classical Merchant-based cutting theories, which typically assume Fc as the dominant component. This inversion is a strong indicator of a shift from a shearing-dominant to a friction-dominant or 'plowing' regime at the tool-chip interface. From a critical standpoint, this behavior in materials like AlMg5 suggests that at ultra-high speeds, the lubricating effect of thermal softening may reduce the shear strength so drastically that the mechanical resistance to the tool's penetration (the thrust component) becomes the bottleneck of the process. This raises a significant concern for tool path planning: if the force vector's directionality flips during a high-speed pass, the resulting change in tool deflection can lead to unexpected dimensional inaccuracies, even if the absolute force magnitude remains low.

3.3.3. Material Properties vs. Tool Geometry

Research indicates that there is no linear relationship between a material's bulk mechanical properties and the resulting cutting forces. Instead, the tool edge micro-geometry (radius and honed features) has a dominant impact. While SCD tools show clear transition points to adiabatic shearing, PCD tools may not exhibit these discrete shifts, suggesting that the tool's grain structure and thermal dissipation capacity fundamentally reorganize the stress distribution in the cutting zone [51].

This non-linear behavior is largely attributed to the 'size effect' phenomenon, which becomes predominant in HSM and ultra-precision machining [59]. When the depth of cut is reduced to a scale comparable to the tool edge radius, the effective rake angle becomes strongly negative, leading to an increase in the specific cutting energy [60], a phenomenon experimentally validated in Figure 3 by comparing the force scaling from the macro- (a) to the micro-regime (b). Consequently, the tool's micro-geometry, specifically the honed edge radius and land width, dictates the transition from a shearing-dominant mechanism to a plowing-dominant one. As documented by Brinksmeier et al. [51], the stagnation zone, or dead metal zone, formed in front of a rounded edge acts as a 'virtual tool geometry', effectively increasing the thrust forces and modifying the thermal gradient within the primary shear zone.

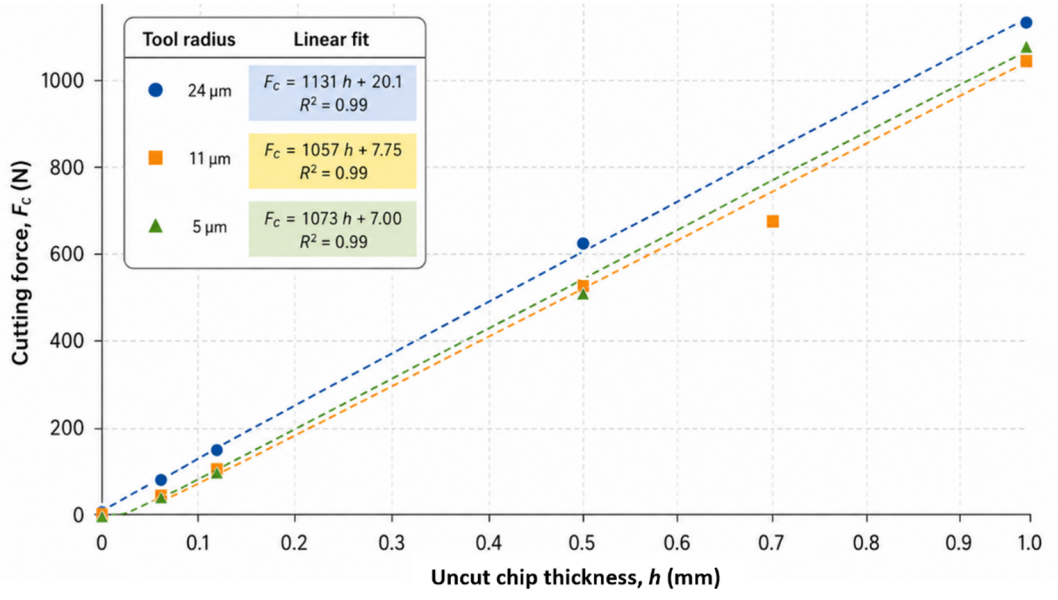


Figure 3. *Cont.*

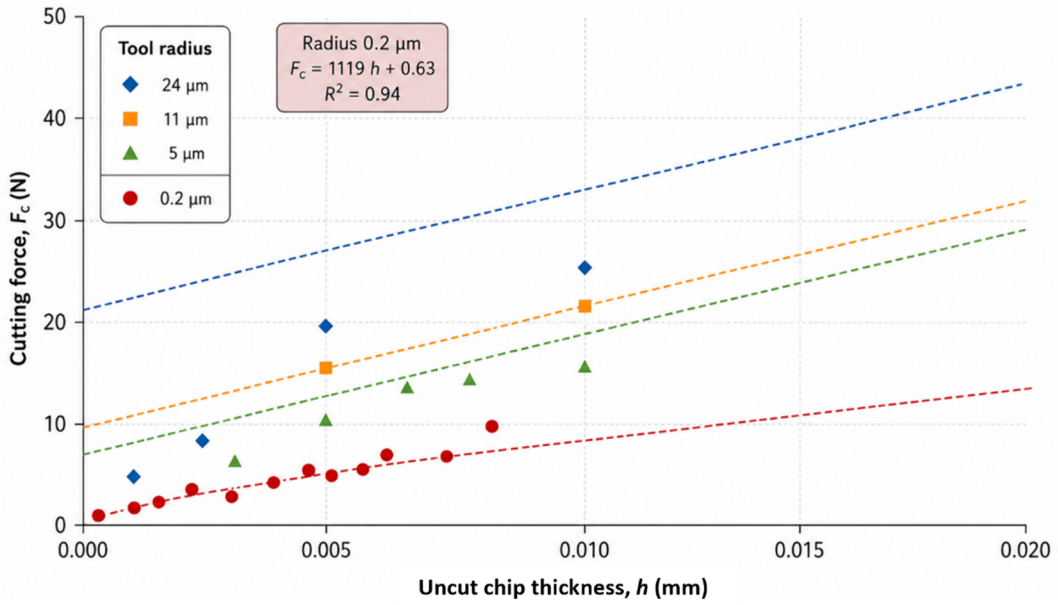


Figure 3. Experimental relationship between cutting forces (Fc) and uncut chip thickness (h) across different scales: (**a**) Macro-scale behavior for tool edge radii between 5 and 24 µm, and (**b**) detailed view of the micro-scale interaction showing the non-linear "Size Effect" for an ultra-sharp edge radius (0.2 µm). Note the difference in the force magnitude and the residual plowing component in the micro-regime. Reproduced from [61].

Furthermore, the thermal dissipation capacity of the tool material plays a synergistic role with its geometry [62]. While Single Crystal Diamond (SCD) tools possess a highly ordered lattice that facilitates rapid phonon-mediated heat conduction, Polycrystalline Diamond (PCD) and Carbide tools introduce grain boundaries that act as thermal barriers [63–66]. This difference in thermal diffusivity explains why SCD tools exhibit sharper transition points to adiabatic shearing; the localized heat is managed differently at the tool-chip interface, preventing the premature thermal softening of the tool itself. Therefore, the selection of tool geometry cannot be decoupled from the tool's material grade, as the combined effect of edge toughness and thermal conductivity determines the stability of the cutting forces and the onset of high-frequency vibrations in the machining of advanced alloys [67,68].

3.4. Synergy between Tool Coatings, Lubrication, and Force Dynamics

The integration of advanced coatings in HSM is not merely a method for wear reduction but a strategic tool for manipulating cutting force dynamics [69,70]. Coated carbides exhibit superior hardness, reduced surface roughness, and lower thermal conductivity compared to uncoated counterparts, creating a chemical barrier that minimizes affinity with the workpiece [71]. To optimize these interfaces, advanced pretreatments such as plasma electrolytic polishing (PEP) have been employed to enhance coating adhesion and promote a more stable tribological contact [72].

The mechanical performance of these coatings is fundamentally tied to their ability to redefine the secondary shear zone. In high-speed regimes, the contact between the chip and the tool rake face is characterized by extreme sticking and sliding zones [73]. Advanced nanostructured coatings, particularly those utilizing transition metal nitrides (TMNs), act as a solid lubricant that reduces the shear strength at this interface [74,75]. This reduction directly translates into lower tangential forces and a decrease in the total energy consumed during chip formation. Moreover, the multilayer architecture of modern coatings, for example in Figure 4, often alternating between hard and ductile nanolayers, serves to dissipate crack energy, preventing the delamination that typically occurs under the cyclic mechanical loading of interrupted cutting operations [76].

Beyond mechanical protection, the thermal management provided by these coatings is a decisive factor in force stabilization. High-speed machining of aerospace alloys frequently generates temperatures exceeding 1000 °C at the cutting edge [77]. Coatings with high oxidation resistance, such as AlTiN or AlCrN, form a stable, protective aluminum oxide (Al_2O_3) layer during the process [78–80]. This 'self-healing' oxide film further reduces the coefficient of friction and acts as a thermal insulator, forcing the generated heat into the chip rather than the tool substrate. This phenomenon maintains the tool's substrate hardness and prevents the catastrophic thermal softening that would otherwise lead to erratic force spikes and dimensional instability.

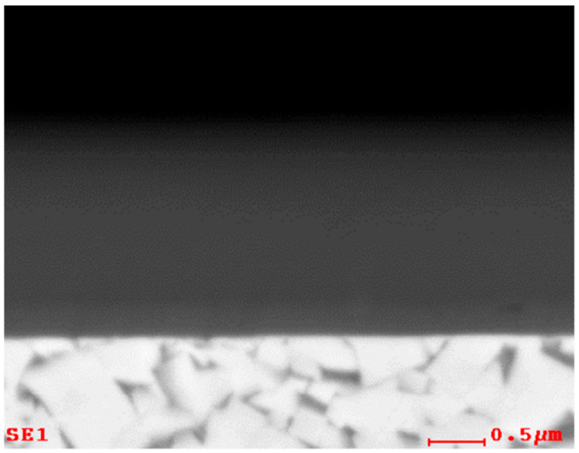


Figure 4. Scanning Electron Microscopy (SEM) cross-sectional micrograph of a nanostructured coating architecture. The image reveals the interface between the bright, textured cemented carbide substrate and the dark, finely layered coating structure, illustrating the nanoscale architecture (reference scale: 0.5 µm) designed for crack energy dissipation and thermal management during HSM. Reproduced from [76].

Finally, the synergy between coating chemistry and tool micro-geometry must be addressed to fully understand force manipulation [81]. A critical "conflict of interest" emerges between coating thickness (needed for thermal/wear protection) and the size effect (which penalizes any increase in effective edge radius). The application of a coating inherently alters the cutting-edge radius often referred to as 'edge rounding'. In low-feed or micro-finishing conditions, where the undeformed chip thickness approaches the edge radius, a thicker protective layer effectively increases the radius and drives the effective rake angle more negative, expanding the stagnation/dead-metal zone. As a result, the process can shift from shearing toward plowing, and the thrust/normal component may increase even when friction at the rake face is reduced by lubricious oxides or near-dry lubrication. If not precisely controlled, an excessively thick coating can increase the plowing effect, paradoxically raising the thrust forces despite the lower friction. This trade-off implies that "best" coatings for wear (thicker, more insulating) are not necessarily "best" for force stability in size-effect-dominated regimes, and therefore coating selection must be co-optimized with feed, edge preparation, and lubrication strategy. Therefore, state-of-the-art research emphasizes the importance of post-coating treatments, such as drag finishing or micro-blasting, to restore the optimal edge sharpness [82,83]. This holistic approach, combining plasma pretreatment, tailored nanostructured layers, and post-process edge calibration, represents the current frontier in achieving predictable and minimized cutting forces in the most demanding HSM environments [84,85].

3.4.1. Nanostructured Coatings and Lubrication Mechanisms

Recent advancements, such as the nanostructured Zr-ZrN-(Zr,Al,Si)N coatings investigated by Vereschaka et al. [86], demonstrate that nanolayering significantly extends tool life by preventing crack propagation and reducing heat transfer. This is particularly relevant in near-dry machining (NDM) or minimum quantity lubrication (MQL) environments. Research using modified Oxley's approaches and boundary lubrication models suggests that in NDM, the lubricating effect has a more profound impact on force reduction (averaging 10% to 20%) than the cooling effect alone [31]. However, these alternative force/friction models have not yet achieved universal industrial adoption because their predictive advantage is often conditional on careful calibration and on inputs that are difficult to standardize across production lines. In practice, parameters governing contact length, heat partition, and boundary-film effectiveness depend strongly on tool micro-geometry, coating chemistry/topography, and delivery of the lubricant (droplet size, impingement, and penetration), which vary with machine-tool enclosure, nozzle configuration, and wear state. This creates an identifiability problem: different parameter sets can reproduce similar force trends, but yield different wear and temperature predictions, reducing trust for process qualification. Moreover, industrial implementation requires low-latency, robust models that can be integrated into CAM/Digital-Twin workflows; many physics-informed friction formulations increase computational burden and demand validation datasets (force + temperature + wear) that are still inconsistently reported in the literature. For difficult-to-cut materials like Inconel 718, the adoption of AlTiN coatings under dry conditions has proven to be an effective strategy for maintaining cutting forces at safe levels while ensuring surface integrity, effectively supporting the industry's shift toward environmentally sustainable manufacturing [87,88].

The challenge of machining Inconel 718 lies primarily in its exceptional mechanical properties at elevated temperatures [89]. As emphasized by Kuo et al. [13], the high strength, poor thermal diffusivity, and rapid work-hardening characteristics of this nickel-based superalloy often result in significantly higher cutting forces and reduced tool efficiency compared to standard alloys like AISI 4340. These intrinsic material properties necessitate a precise optimization of the tool's cutting edge to mitigate surface damage. In this regard, the experimental investigation by Pawade et al. [90] in high-speed turning revealed that the main cutting force component can be two to three times greater than the feed and radial forces. Their study highlights that a honed plus chamfered edge geometry is instrumental in reducing these forces, as higher force levels are directly correlated with poor surface finish and extensive microstructural damage.

Furthermore, the quest for cleaner manufacturing has led to a critical evaluation of cooling strategies specifically for this superalloy. While dry cutting is often the goal, the low cooling capacity of air can be a limiting factor. To address this, Zhang & Wang [91] explored the performance of Minimum Quantity Cooling Lubrication (MQCL), which combines cryogenic air with biodegradable vegetable oil. Their findings demonstrate that MQCL significantly outperforms both dry and conventional MQL conditions, effectively reducing cutting forces and extending tool life. By establishing a clear relationship between tool wear propagation and force variations, this research confirms that MQCL provides a viable, environmentally friendly alternative for the high-speed milling of Inconel 718, balancing technical performance with the increasing demands for sustainable production. This synergy between cryogenic cooling and oil-mist lubrication, resulting in the lowest wear rates compared to isolated strategies, is schematically represented in Figure 5.

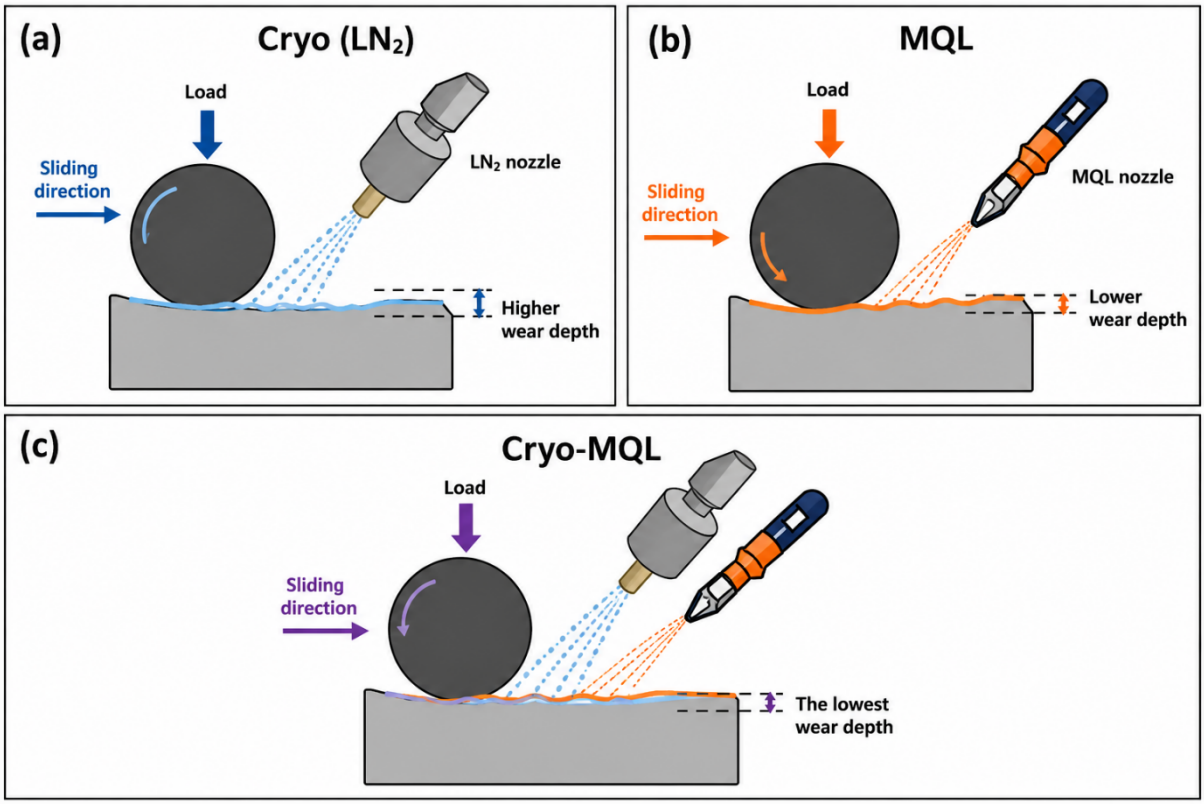


Figure 5. Schematic representation of the synergistic effects of different cooling and lubrication strategies on tool-workpiece interaction: (**a**) Cryogenic cooling (liquid nitrogen (LN_2)), (**b**) Minimum Quantity Lubrication (MQL), and (**c**) Hybrid Cryo-MQL approach. The diagram highlights the significant reduction in wear depth achieved through the combination of thermal management and boundary lubrication. Reproduced from [92].

3.4.2. Comparative Analysis: Inconel 718 vs. Ti–6Al–4V

A critical aspect of HSM is the material-specific response to cutting parameters. While both Titanium alloys (Ti–6Al–4V) and Nickel-based superalloys (Inconel 718) exhibit a decrease in resultant forces as cutting speeds increase, due to the thermal softening effect, the absolute force levels in Inconel 718 are consistently higher under identical conditions [93]. This disparity is quantified through the force ratio (Fc/thrust force, F_t), which serves as a vital indicator of the tool's tribological behavior and the efficiency of the shearing process [94].

The fundamental divergence in force magnitude between these two aerospace alloys is primarily governed by their distinct thermal properties and hardening mechanisms. In the case of Ti–6Al–4V, its remarkably low thermal conductivity causes a high concentration of heat at the cutting edge, which, despite accelerating tool wear, promotes an intense thermal softening that significantly lowers the shear strength of the material during high-speed passes [95]. In contrast, Inconel 718 maintains much of its mechanical strength at elevated temperatures due to the presence of the precipitating phase [96]. This metallurgical stability, combined with a high work-hardening rate, ensures that the energy required for plastic deformation remains elevated even as cutting speeds approach the HSM regime, resulting in the higher absolute force levels observed in empirical studies.

Furthermore, the chip formation morphology plays a decisive role in the oscillation and stability of the cutting forces [97,98]. Machining Ti–6Al–4V typically results in the formation of serrated or 'saw-tooth' chips due to localized adiabatic shear banding [99,100]. This phenomenon creates a high-frequency cyclic variation in the cutting forces, which requires high-bandwidth dynamometry for accurate capture. For Inconel 718, while chip segmentation also occurs, the high chemical affinity between the Nickel matrix and the tool substrate often leads to the formation of a Built-Up Edge (BUE) or intense adhesive layers [101,102]. These adhesive interactions increase the friction coefficient at the rake face, further inflating the thrust force and altering the Fc/Ft ratio, which serves as a proxy for cutting efficiency and the onset of tool degradation.

Finally, the transition toward sustainable machining through Minimum Quantity Cooling Lubrication (MQCL) or cryogenic assistance has shown different degrees of effectiveness for each material [103]. For Titanium alloys, the primary goal of the cooling medium is to prevent the rapid chemical diffusion between the Ti-matrix and the tool. However, for Inconel 718, the strategy shifts toward managing the extreme mechanical loads. Research indicates that while cryogenic cooling can drastically reduce the tool-chip interface temperature, it may paradoxically increase the cutting forces in Inconel due to the suppression of the thermal softening effect [104,105]. Therefore, the selection of the optimal cutting speed must be carefully balanced with the cooling strategy to ensure that the reduction in force achieved through speed-induced softening is not negated by the increased material hardness at low temperatures.

3.4.3. Influence of Tool Path Strategies in Mold Manufacturing

Beyond material properties, the kinematics of the tool path during complex operations, such as pocket opening, represent a major challenge due to force spikes and rapid tool degradation. Comparative studies of entry strategies reveal that while Strategies I and II (Ramp and Helical entries) exhibit a more progressive force increase in the direction perpendicular to the flank wear, they are still characterized by sharp peaks at trajectory transition points, which can compromise dimensional accuracy. In contrast, Strategy III (Plunge Entry) often leads to catastrophic tool fracture due to the high probability of chip recutting, resulting in erratic and extremely high root mean square (RMS) force values that jeopardize machining stability. These vibration patterns and force fluctuations highlight the critical necessity for a deeper understanding of the dynamic behavior of cutting forces in mold making; consequently, future investigations must focus on synchronizing tool path algorithms with real-time force feedback to prevent chatter, mitigate tool wear, and ensure the structural integrity of high-precision components [106].

The comparative analysis of these strategies indicates that the stability of cutting forces in mold manufacturing is intrinsically linked to the tool–workpiece engagement (TWE) [107]. While ramp and helical entries distribute the mechanical load more uniformly, the force spikes observed at trajectory transitions suggest a transient loss of the steady-state cutting condition, which can trigger self-excited vibrations (chatter). Conversely, the failure of Strategy III (Plunge Entry) underscores the dangers of chip evacuation interference; when chips are recut in a confined zone, the resulting stochastic force impulses exceed the tool's rupture strength. Therefore, the optimization of HSM for complex geometries requires a holistic approach that goes beyond selecting cutting parameters. It demands a synergy between adaptive tool-path algorithms and the previously discussed nanostructured coatings, as a coating with high impact resistance and low friction can partially mitigate the damaging effects of force peaks during critical entry moves. This integration represents a vital frontier for achieving zero-defect manufacturing in high-precision mold industries.

3.5. Fundamental Kinematics and Geometric Parameters in HSM

The interaction between the cutting tool and the workpiece is governed by a set of instantaneous parameters that dictate the material removal rate (MRR) and the resulting force vectors. The primary variables, depth of cut (a_p), feed (f), and cutting speed (v_c), form the basis for any analytical or numerical prediction of the machining process [29]. In the High-Speed Machining (HSM) regime, these parameters do not act in isolation; their selection

directly influences the strain rate and the adiabatic heating of the shear zone, which in turn alters the specific cutting pressure (k_c) and the overall stability of the operation.

The coupling of these parameters defines the undeformed chip thickness, which is arguably the most critical variable in determining the magnitude of the cutting force vectors [108]. In milling operations, particularly in HSM, this thickness is not constant but varies sinusoidally as the tool rotates, requiring a dynamic approach to force modeling [109,110]. As the feed and depth of cut increase, the cross-sectional area of the chip grows, leading to a proportional rise in the mechanical load on the tool's rake face [111,112]. However, in the high-speed regime, the increase in cutting speed induces a nonlinear response: the intense localized heat reduces the material's yield strength faster than the strain-hardening effect can increase it [113,114]. This delicate balance between the geometric parameters and the thermoplastic behavior of the workpiece is what ultimately dictates the specific cutting pressure, making the precise selection of parameters the primary mechanism for controlling tool vibration and ensuring surface integrity.

This kinematic interaction manifests in distinct ways depending on the chosen manufacturing process. In turning, the workpiece rotation determines the cutting speed, while the tool executes two primary movements: penetration, which defines the depth of cut, and feed, establishing the axial displacement per revolution [115]. Conversely, milling operations (radial and end milling) shift the cutting speed responsibility to the tool's rotation and diameter. In radial milling, the engagement is characterized by the cutting width, whereas in end milling, the depth of cut is often limited by the effective flute length or the height of the mounted inserts. The actual volumetric removal is governed by the feed rate, which is the product of the feed and the spindle speed, directly impacting the total machining time. For multi-insert tools, the feed per tooth becomes the critical variable for calculating the chip load, ensuring that only a specific portion of the cutting edge encounters the workpiece at any given instant.

The geometric foundation of force generation lies in the cutting area, which, in its simplest orthogonal form, is the product of the depth of cut and the feed. By integrating the material-specific cutting pressure, the tangential cutting force can be analytically estimated. However, a critical discussion of these parameters in the HSM context reveals that they do not function as static variables. While traditional models treat kc as a constant, in high-speed regimes, it becomes highly sensitive to the nonlinear coupling between thermal softening and strain-rate effects. As vc increases, localized adiabatic heating reduces the material's yield strength, effectively lowering kc and the resulting Fc. On the other hand, if the feed (f) is reduced to values comparable to the tool's edge radius, the size effect takes over, increasing the specific energy required for chip formation due to a predominantly negative effective rake angle. Therefore, ideal parameter selection in HSM is not merely a productivity calculation but a strategic balance: maintaining sufficient chip thickness to avoid the size effect while leveraging high speeds to trigger the thermal softening necessary for force reduction and surface integrity preservation [116,117].

3.6. Strategic Analysis of HSM Implementation: A SWOT Perspective

To synthesize the technical findings discussed in this study, a SWOT analysis (Figure 6) is presented to evaluate the internal and external factors influencing the adoption of High-Speed Machining (HSM) in high-performance industries, such as aerospace and mold making.

The SWOT analysis provides a holistic overview of the industrial feasibility and strategic positioning of High-Speed Machining. To strengthen its review value, the SWOT discussion can be anchored to core outcome indicators—cutting force (level and stability), tool wear (rate and mode), and surface integrity (roughness, residual stresses, sub-surface damage)—because these metrics ultimately govern productivity, quality, and cost. A critical assessment of the Strengths reveals that the primary driver for HSM adoption remains the synergistic relationship between productivity and force dynamics. By leveraging the thermal softening effect, manufacturers can achieve a higher Material Removal Rate (MRR) without a linear increase in mechanical load on the machine spindle. This advantage is particularly decisive in the production of thin-walled aerospace components, where traditional machining forces would cause unacceptable part deflection and dimensional errors.

However, the Weaknesses highlighted—specifically accelerated tool wear and process sensitivity—suggest that the economic viability of HSM is heavily dependent on the "technological maturity" of the manufacturing facility. The requirement for advanced modal analysis to mitigate chatter, coupled with the necessity for expensive nanostructured coatings, creates a narrow operational window. In indicator terms, these weaknesses manifest as higher scatter in force signatures (reduced stability margins), faster wear progression that changes the effective edge geometry, and a tighter link between transient force peaks and surface/sub-surface damage. Moreover, a balanced sustainability view should consider a "total footprint" perspective: while NDM/MQCL can reduce in-process fluid consumption, the upstream energy and material intensity of producing advanced multilayer coatings (and associated pretreatments/post-treatments) can be non-negligible, meaning that the net environmental benefit

depends on whether coating-enabled tool-life extension and scrap reduction outweigh the coating production burden. This implies that without the advanced FEM modeling and real-time monitoring discussed in previous sections, the internal strengths of HSM may be negated by the high costs of premature tool failure and machine downtime. Thus, the transition from conventional to high-speed machining is not merely a change in spindle speed, but a fundamental shift toward a data-driven manufacturing environment.



Figure 6. SWOT analysis of High-Speed Machining implementation in industrial environments.

Looking at the external environment, the Opportunities for Digital Twin integration and sustainable practices (MQCL) represent the next frontier for the industry. The ability to simulate the cutting zone with high fidelity allows for the mitigation of the Threats posed by alternative technologies like Additive Manufacturing, which, while capable of complex geometries, often lacks the surface integrity and tight tolerances inherent to HSM. To move beyond a visionary statement, a latency-aware roadmap is required: complex multi-physics FEM may require hours for convergence, whereas real-time control acts on millisecond-to-second horizons. Practical industrial approaches therefore rely on hierarchical Digital Twins, where (i) offline, high-fidelity FEM is used for design-of-experiments, parameter bounding, and generation of training/validation datasets; (ii) reduced-order or surrogate models (response surfaces, calibrated mechanistic models, or ML emulators) run online to estimate forces/temperatures within the control loop; and (iii) periodic re-calibration closes the gap as tools wear and boundary conditions drift. Ultimately, the successful implementation of HSM for "difficult-to-cut" materials such as Inconel 718 depends on the strategic mitigation of high initial investments through superior process stability and the cultivation of a highly skilled workforce capable of interpreting complex force-path dynamics.

3.7. Integrative Discussion: Thermomechanical Stability and Strategic Viability

The fundamental challenge in High-Speed Machining (HSM) of advanced alloys like Inconel 718 and Ti–6Al–4V lies in the management of the thermal-gradient interface. As synthesized from the reviewed literature, the HSM process operates as a "double-edged sword": the cutting speed must be high enough to trigger the adiabatic

shearing required for thermal softening, thereby reducing cutting forces, yet controlled enough to inhibit the kinetics of rapid tool degradation.

The transition from machining conventional steels to Nickel-based superalloys highlights a shift in the deformation mechanisms. In the former, the high thermal diffusivity allows for a relatively wide processing window. In the latter, however, the discussion is dominated by low thermal conductivity and high work-hardening rates. The consensus among authors points to a critical thermal threshold; exceeding this limit triggers a transition from stable shearing to catastrophic adhesive wear, regardless of the refined micro-geometry achieved through honed edges. Crucial to this metallurgical evolution is the distinct nature of the dynamic recrystallization (DRX) occurring in the primary shear zone. In Titanium alloys, the microstructure is refined via localized shear banding, whereas Inconel 718 exhibits a coupled mechanism between strain-induced hardening and thermal softening, which dictates the fluctuating nature of the force ratio (Fc/Ft).

The reported 10% to 20% force reduction in Near Dry Machining (NDM) must be interpreted within the context of the Size Effect. For micro-feeds comparable to the tool edge radius, the effective rake angle becomes strongly negative, generating a continuous "plowing" path that compromises surface integrity. This suggests that the lubricating mechanism in MQCL is not merely a function of cooling, but of reducing the stagnation zone (dead metal zone) in front of the tool, effectively "sharpening" the virtual tool geometry.

A recurring theme in the HSM of these alloys is the asymmetric thermal distribution. Because the tool interacts with materials of vastly different chemical affinities, the "heat partitioning" is never uniform. This is particularly evident in coated carbide tools, where Functional Drift, characterized by the oxidation of the AlTiN layer into Al_2O_3, acts as a protective barrier. By utilizing nanostructured coatings, researchers have managed to optimize heat dissipation, forcing the thermal energy into the chip rather than the tool substrate. This strategic choice, however, introduces the threat of coating delamination under cyclic mechanical loading, creating a direct conflict between high productivity (MRR) and tool cost-effectiveness.

Perhaps the most sophisticated aspect of this discussion is the preservation of sub-surface integrity. The research indicates that the future of HSM lies in a multi-stage approach: utilizing optimized tool-path strategies (like spiral ramp entries) to mitigate initial force spikes, followed by real-time monitoring to "tune" the final surface properties. The move toward Digital Twin integration, identified in the SWOT analysis, is a consequence of the need to predict these complex thermomechanical interactions. Therefore, the discussion moves beyond simple force reduction toward process reliability, ensuring that high-speed manufacturing remains a viable and sustainable alternative for the next generation of aerospace components.

4. Conclusions

This review consolidates dispersed evidence on how coating architecture and process parameters jointly shape cutting-force generation in High-Speed Machining (HSM), and proposes an integrated "coating–parameter–wear" framework that connects (i) tribological mechanisms at the tool–chip interface, (ii) force-vector evolution, and (iii) tool degradation pathways. Based on the integrated analysis of metallurgical integrity, tool geometry, lubrication, and strategic viability, the following conclusions are drawn:

- Dominance of Tool Micro-geometry: Research confirms that there is no linear correlation between bulk material properties and cutting forces in HSM. Instead, the tool edge micro-geometry (honed radius and rake angle) dictates the transition from a shearing-dominant to a plowing-dominant regime. This work clarifies that the "size effect" is the mechanistic bridge between geometry and force amplification at micro-feeds, and therefore the primary lever for controlling force sensitivity when feeds approach the edge-radius scale.
- Thermal Softening vs. Strain Hardening: In the machining of difficult-to-cut alloys like Inconel 718 and Ti–6Al–4V, the utilization of high cutting speeds triggers adiabatic shearing. At the cutting edge, reported temperatures frequently exceed 1000 °C, and for Ti–6Al–4V the low thermal conductivity can drive a large heat partition into the tool (≈80% as reported in the reviewed literature), promoting localized thermal softening that counteracts work hardening and contributes to force reduction and process stability.
- Synergy of Nanostructured Coatings and Near-Dry Strategies: The implementation of advanced coatings (e.g., AlTiN, Zr-based nitrides) combined with near-dry approaches (NDM/MQCL) provides a viable pathway toward sustainable machining. Across the reviewed studies, near-dry machining is associated with an average 10% to 20% reduction in cutting forces compared to dry baselines, with the dominant contribution arising from boundary-lubrication effects rather than bulk cooling alone. This synthesis advances understanding by explicitly linking coating-driven heat partitioning (e.g., AlTiN → Al_2O_3 "self-healing" layers) with lubricant penetration and the resulting force-vector stability.

- Kinematic Strategy and Force Stability: The analysis of tool-path strategies for mold manufacturing reveals that ramp and helical entries provide a more stable force distribution than plunge entries, which are prone to catastrophic failure due to chip recutting. The reviewed evidence indicates that trajectory transitions can dominate the force signature via transient peaks and elevated RMS levels, making tool–workpiece engagement (TWE) a practical descriptor for predicting when stability is lost. Accordingly, progress in understanding is achieved by positioning entry kinematics as a first-order contributor to force dynamics (alongside coatings and lubrication), rather than a secondary CAM choice.
- Strategic Industrial Viability and Modeling Reliability: As synthesized in the SWOT analysis, the future of HSM lies in the integration of Digital Twins and FEM modeling to move from reactive trial-and-error to predictive process design. However, the reviewed evidence also shows that FEM-based force predictions can deviate substantially when constitutive parameters are transferred from standard tests; the "calibration gap" reported for SHPB-derived Johnson-Cook parameters can produce ~20–30% error in predicted cutting forces if not tuned against high-frequency experimental benchmarks. This underscores that the progress in knowledge is not only "more modeling," but better coupled model–measurement workflows (dynamometry/AE + calibrated FEM) for dependable force control.

Limitations: This is a narrative review and therefore inherits limitations of the underlying literature, including heterogeneous cutting conditions (tool geometry, engagement, and parameter definitions), inconsistent reporting of force components and bandwidth, and limited cross-study comparability of coating architectures and post-treatment states. In addition, many studies quantify "force reduction" without simultaneously reporting tool wear evolution and surface/sub-surface integrity, restricting the ability to derive universally transferable optimization rules. Outlook: Future work should prioritize standardized reporting of force vectors (including Fc/Ft trends), explicit characterization of tool–workpiece engagement (TWE), and closed-loop validation pipelines that fuse high-frequency dynamometry/AE with calibrated multi-physics FEM. Such efforts will strengthen the proposed coating–parameter–wear framework and accelerate translation toward robust, sustainable, zero-defect HSM of difficult-to-cut alloys.

Author Contributions

N.P.V.S., R.S.-C. and W.D.: conceptualization; N.P.V.S., R.B.C. and W.D.: methodology; N.P.V.S., A.B. and G.P.: data curation, visualization; N.P.V.S.: writing—original draft preparation; N.P.V.S.: investigation; R.S.-C. and R.B.C.: supervision; W.D. and R.D.C.: validation; R.D.C.: writing—reviewing and editing. All authors have read and agreed to the published version of the manuscript.

Funding

The work was developed under the "DRIVOLUTION—Transition to the factory of the future", Research Project Code 02/C05-i01.02/2022, Project no. 23, supported by European Structural and Investments Funds with the "Portugal2020" program scope.

Data Availability Statement

Not applicable.

Conflicts of Interest

The authors declare no conflict of interest.

Use of AI and AI-Assisted Technologies

During the preparation of this work, the authors used ChatGPT to support English language editing, improve grammatical accuracy and readability, and assist in verifying appropriate technical terminology and expressions. After using this tool, the authors reviewed and edited the content as needed and take full responsibility for the content of the published article.

References

1. Sebbe, N.P.V.; Fernandes, F.; Sousa, V.F.C.; et al. Hybrid Manufacturing Processes Used in the Production of Complex Parts: A Comprehensive Review. *Metals* **2022**, *12*, 1874. https://doi.org/10.3390/met12111874.

2. Adin, M.Ş. Machining aerospace aluminium alloy with cryo-treated and untreated HSS cutting tools. *Adv. Mater. Process. Technol.* **2024**, *10*, 2664–2689. https://doi.org/10.1080/2374068X.2023.2273035.
3. Liang, X.; Liu, Z. Tool wear behaviors and corresponding machined surface topography during high-speed machining of Ti–6Al–4V with fine grain tools. *Tribol. Int.* **2018**, *121*, 321–332. https://doi.org/10.1016/j.triboint.2018.01.057.
4. Zhao, G.; Zhao, B.; Ding, W.; et al. Nontraditional energy-assisted mechanical machining of difficult-to-cut materials and components in aerospace community: A comparative analysis. *Int. J. Extrem. Manuf.* **2024**, *6*, 022007. https://doi.org/10.1088/2631-7990/ad16d6.
5. Raghavendra, S.; Sathyanarayana, P.S.; S, S.; et al. High speed machining of titanium Ti-6Al-4V alloy components: Study and optimisation of cutting parameters using RSM. *Adv. Mater. Process. Technol.* **2022**, *8*, 277–290. https://doi.org/10.1080/2374068X.2020.1806684.
6. Sebbe, N.P.V.; Silva, F.J.G.; Durão, L.M.; et al. Comparative Analysis of the Wear Behavior of TiN/TiAlN-, TiAlVN-, and TiAlYN-Coated Tools in Milling Operations of Inconel 718. *J. Tribol.* **2025**, *147*, 074202. https://doi.org/10.1115/1.4066954.
7. Pedroso, A.F.V.; Sousa, V.F.C.; Sebbe, N.P.V.; et al. A Comprehensive Review on the Conventional and Non-Conventional Machining and Tool-Wear Mechanisms of INCONEL®. *Metals* **2023**, *13*, 585. https://doi.org/10.3390/met13030585.
8. Sebbe, N.P.V.; Fernandes, F.; Silva, F.J.; et al. Wear Behavior Analysis of TiN/TiAlN Coated Tools in Milling of Inconel 718. In *Flexible Automation and Intelligent Manufacturing: Establishing Bridges for More Sustainable Manufacturing Systems*; Springer: Cham, Switzerland, 2024; pp. 784–795. https://doi.org/10.1007/978-3-031-38241-3_87.
9. Freitas, F.R.S.; Casais, R.C.B.; Silva, F.J.G.; et al. Wear Behavior of TiAlN/DLC Coating on Tools in Milling Copper–Beryllium Alloy AMPCOLOY® 83. *Coatings* **2024**, *14*, 1354. https://doi.org/10.3390/coatings14111354.
10. Dabees, S.; Mirzaei, S.; Kaspar, P.; et al. Characterization and Evaluation of Engineered Coating Techniques for Different Cutting Tools—Review. *Materials* **2022**, *15*, 5633. https://doi.org/10.3390/ma15165633.
11. Ganeshkumar, S.; Venkatesh, S.; Paranthaman, P.; et al. Performance of Multilayered Nanocoated Cutting Tools in High-Speed Machining: A Review. *Int. J. Photoenergy* **2022**, *2022*, 5996061. https://doi.org/10.1155/2022/5996061.
12. Guo, H.; Zhang, Y.; Zhu, K. Interpretable deep learning approach for tool wear monitoring in high-speed milling. *Comput. Ind.* **2022**, *138*, 103638. https://doi.org/10.1016/j.compind.2022.103638.
13. Kuo, C.-P.; Ling, C.-C.; Chen, S.-H.; et al. The prediction of cutting force in milling Inconel-718. *Int. J. Adv. Manuf. Technol.* **2006**, *27*, 655–660. https://doi.org/10.1007/s00170-004-2257-6.
14. Sebbe, N.P.V.; Fernandes, F.; Silva, F.J.G.; et al. Wear Behavior of TiAlVN-Coated Tools in Milling Operations of INCONEL® 718. *Coatings* **2024**, *14*, 311. https://doi.org/10.3390/coatings14030311.
15. Dehghan, S.; Soury, E.; Ismail, M.I.S. A comparative study on machining and tool performance in friction drilling of difficult-to-machine materials AISI304, Ti–6Al–4V, Inconel718. *J. Manuf. Process.* **2021**, *61*, 128–152. https://doi.org/10.1016/j.jmapro.2020.10.078.
16. Alauddin, M.; El Baradie, M.A.; Hashmi, M.S.J. End-Milling Machinability of Inconel 718. *Proc. Inst. Mech. Eng. Part B J. Eng. Manuf.* **1996**, *210*, 11–23. https://doi.org/10.1243/PIME_PROC_1996_210_082_02.
17. Roy, S.; Kumar, R.; Panda, A.; et al. A Brief Review on Machining of Inconel 718. *Mater. Today Proc.* **2018**, *5 Pt 3*, 18664–18673. https://doi.org/10.1016/j.matpr.2018.06.212.
18. Feng, Y.; Pan, Z.; Liang, S.Y. Temperature prediction in Inconel 718 milling with microstructure evolution. *Int. J. Adv. Manuf. Technol.* **2018**, *95*, 4607–4621. https://doi.org/10.1007/s00170-018-1581-1.
19. Kamdani, K.; Hasan, S.; Lajis, M.A. The Effects of TiAlN and TiN Coating during End Milling of INCONEL 718. *Appl. Mech. Mater.* **2014**, *564*, 566–571. https://doi.org/10.4028/www.scientific.net/AMM.564.566.
20. Cantero, J.L.; Díaz-Álvarez, J.; Infante-García, D.; et al. High Speed Finish Turning of Inconel 718 Using PCBN Tools under Dry Conditions. *Metals* **2018**, *8*, 192. https://doi.org/10.3390/met8030192.
21. Oosthuizen, T.; Nunco, K.; Conradie, P.; et al. The effect of cutting parameters on surface integrity in milling TI6AL4V. *S. Afr. J. Ind. Eng.* **2016**, *27*, 115–123. https://doi.org/10.7166/27-4-1199.
22. Fernández-Vidal, S.R.; Mayuet, P.; Rivero, A.; et al. Analysis of the Effects of Tool Wear on Dry Helical Milling of Ti6Al4V Alloy. *Procedia Eng.* **2015**, *132*, 593–599. https://doi.org/10.1016/j.proeng.2015.12.536.
23. Khanna, N.; Airao, J.; Kshitij, G.; et al. Sustainability analysis of new hybrid cooling/lubrication strategies during machining Ti6Al4V and Inconel 718 alloys. *Sustain. Mater. Technol.* **2023**, *36*, e00606. https://doi.org/10.1016/j.susmat.2023.e00606.
24. Sebbe, N.P.V.; Silva, F.J.G.; Pinto, A.; et al. Exploring Post-Processing Operations of Ti Alloys Using Hybrid Manufacturing Systems. *J. Mech. Eng. Manuf.* **2026**, *2*, 9. https://doi.org/10.53941/jmem.2026.100009.
25. da Silva, R.B.; Machado, Á.R.; Ezugwu, E.O.; et al. Tool life and wear mechanisms in high speed machining of Ti–6Al–4V alloy with PCD tools under various coolant pressures. *J. Mater. Process. Technol.* **2013**, *213*, 1459–1464. https://doi.org/10.1016/j.jmatprotec.2013.03.008.
26. Sousa, V.; Silva, F.J.G.; Fecheira, J.S.; et al. Accessing the cutting forces in machining processes: An overview. *Procedia Manuf.* **2020**, *51*, 787–794. https://doi.org/10.1016/j.promfg.2020.10.110.

27. Guimarães, B.M.P.; da Silva Fernandes, C.M.; de Figueiredo, D.A.; et al. Cutting temperature measurement and prediction in machining processes: Comprehensive review and future perspectives. *Int. J. Adv. Manuf. Technol.* **2022**, *120*, 2849–2878. https://doi.org/10.1007/s00170-022-08957-z.
28. Khadka, S.; Rahman Rashid, R.A.; Stephens, G.; et al. Predicting cutting tool life: Models, modelling, and monitoring. *Int. J. Adv. Manuf. Technol.* **2025**, *136*, 3037–3076. https://doi.org/10.1007/s00170-024-14961-2.
29. Bremer, F.; Matthiesen, S. High-speed cutting with involute blades: Experimental research on cutting forces. *J. Food Eng.* **2021**, *293*, 110380. https://doi.org/10.1016/j.jfoodeng.2020.110380.
30. Sousa, V.F.C.; Silva, F.J.G. Recent Advances on Coated Milling Tool Technology—A Comprehensive Review. *Coatings* **2020**, *10*, 235. https://doi.org/10.3390/coatings10030235.
31. Li, K.-M.; Liang, S.Y. Modeling of cutting forces in near dry machining under tool wear effect. *Int. J. Mach. Tools Manuf.* **2007**, *47*, 1292–1301. https://doi.org/10.1016/j.ijmachtools.2006.08.017.
32. Haber, R.E.; Jiménez, J.E.; Peres, C.R.; et al. An investigation of tool-wear monitoring in a high-speed machining process. *Sens. Actuators A Phys.* **2004**, *116*, 539–545. https://doi.org/10.1016/j.sna.2004.05.017.
33. Markopoulos, A.P.; Kantzavelos, K.; Galanis, N.I.; et al. 3D Finite Element Modeling of High Speed Machining. In *Dynamic Methods and Process Advancements in Mechanical, Manufacturing, and Materials Engineering*; IGI Global: Hershey, PA, USA, 2013; pp. 178–196. https://doi.org/10.4018/978-1-4666-1867-1.ch011.
34. Mostaghimi, H.; Park, C.I.; Kang, G.; et al. Reconstruction of cutting forces through fusion of accelerometer and spindle current signals. *J. Manuf. Process.* **2021**, *68*, 990–1003. https://doi.org/10.1016/j.jmapro.2021.06.007.
35. Zhang, C.; Li, C.; Xu, M.; et al. Cutting force and nonlinear chatter stability of ball-end milling cutter. *Int. J. Adv. Manuf. Technol.* **2022**, *120*, 5885–5908. https://doi.org/10.1007/s00170-022-09150-y.
36. Pedroso, A.F.V.; Sousa, V.F.C.; Sebbe, N.P.V.; et al. A brief review of INCONEL® alloys numerical analysis on traditional machining predictability. *Procedia Comput. Sci.* **2024**, *232*, 1109–1120. https://doi.org/10.1016/j.procs.2024.01.109.
37. Saez-de-Buruaga, M.; Gainza, L.; Aristimuno, P.; et al. FEM modeling of hard turning 42CrMoS4 steel. *Procedia CIRP* **2019**, *82*, 77–82. https://doi.org/10.1016/j.procir.2019.04.059.
38. Jain, A.; Bajpai, V. Introduction to high-speed machining (HSM). In *High Speed Machining*; Elsevier: Amsterdam, The Netherlands, 2020; pp. 1–25. https://doi.org/10.1016/B978-0-12-815020-7.00001-1.
39. Guo, L.; Guo, X.; Lv, F. A Study on Dual-Mode Hybrid Dynamics Finite Element Algorithm for Human Soft Tissue Deformation Simulation. *Symmetry* **2025**, *17*, 765. https://doi.org/10.3390/sym17050765.
40. Zhou, G.; Wang, T.; Jiang, C.; et al. A coupled smoothed finite element method and Lagrangian particle tracking model for three-dimensional dilute particle-laden flows. *Appl. Math. Comput.* **2024**, *475*, 128726. https://doi.org/10.1016/j.amc.2024.128726.
41. Korkmaz, M.E.; Gupta, M.K. A State of the Art on Simulation and Modelling Methods in Machining: Future Prospects and Challenges. *Arch. Comput. Methods Eng.* **2023**, *30*, 161–189. https://doi.org/10.1007/s11831-022-09794-9.
42. Rodriguez, J.M.; Larsson, S.; Carbonell, J.M.; et al. Implicit or explicit time integration schemes in the PFEM modeling of metal cutting processes. *Comput. Part. Mech.* **2022**, *9*, 709–733. https://doi.org/10.1007/s40571-021-00439-5.
43. De Micheli, P.O.; Mocellin, K. 2D high speed machining simulations using a new explicit formulation with linear triangular elements. *Int. J. Mach. Mach. Mater.* **2011**, *9*, 266. https://doi.org/10.1504/IJMMM.2011.039651.
44. Movahhedy, M.R.; Gadala, M.S.; Altintas, Y. Simulation of chip formation in orthogonal metal cutting process: An ale finite element approach. *Mach. Sci. Technol.* **2000**, *4*, 15–42. https://doi.org/10.1080/10940340008945698.
45. Rodríguez, J.M.; Carbonell, J.M.; Jonsén, P. Numerical Methods for the Modelling of Chip Formation. *Arch. Comput. Methods Eng.* **2020**, *27*, 387–412. https://doi.org/10.1007/s11831-018-09313-9.
46. Vaziri, M.R.; Salimi, M.; Mashayekhi, M. Evaluation of chip formation simulation models for material separation in the presence of damage models. *Simul. Model. Pract. Theory* **2011**, *19*, 718–733. https://doi.org/10.1016/j.simpat.2010.09.006.
47. Shuang, F.; Chen, X.; Ma, W. Numerical analysis of chip formation mechanisms in orthogonal cutting of Ti6Al4V alloy based on a CEL model. *Int. J. Mater. Form.* **2018**, *11*, 185–198. https://doi.org/10.1007/s12289-017-1341-z.
48. Chen, B.; Starman, B.; Halilovič, M.; et al. Finite Element Model Updating for Material Model Calibration: A Review and Guide to Practice. *Arch. Comput. Methods Eng.* **2025**, *32*, 2035–2112. https://doi.org/10.1007/s11831-024-10200-9.
49. Du, M.; Cheng, Z.; Wang, S. Finite element modeling of friction at the tool-chip-workpiece interface in high speed machining of Ti6Al4V. *Int. J. Mech. Sci.* **2019**, *163*, 105100. https://doi.org/10.1016/j.ijmecsci.2019.105100.
50. Asad, M. Effects of Tool Edge Geometry on Chip Segmentation and Exit Burr: A Finite Element Approach. *Metals* **2019**, *9*, 1234. https://doi.org/10.3390/met9111234.
51. Brinksmeier, E.; Preuss, W.; Riemer, O.; et al. Cutting forces, tool wear and surface finish in high speed diamond machining. *Precis. Eng.* **2017**, *49*, 293–304. https://doi.org/10.1016/j.precisioneng.2017.02.018.
52. Fujishima, M.; Ohno, K.; Nishikawa, S.; et al. Study of sensing technologies for machine tools. *CIRP J. Manuf. Sci. Technol.* **2016**, *14*, 71–75. https://doi.org/10.1016/j.cirpj.2016.05.005.

53. Sousa, V.F.C.; Silva, F.J.G. Recent Advances in Turning Processes Using Coated Tools—A Comprehensive Review. *Metals* **2020**, *10*, 170. https://doi.org/10.3390/met10020170.
54. Sztankovics, I. Experimental and Analytical Study of Cutting Force Components and Form Errors in Tangential Turning of 42CrMo4 Steel. *J. Exp. Theor. Anal.* **2026**, *4*, 9. https://doi.org/10.3390/jeta4010009.
55. Liang, Q.; Zhang, D.; Wu, W.; et al. Methods and Research for Multi-Component Cutting Force Sensing Devices and Approaches in Machining. *Sensors* **2016**, *16*, 1926. https://doi.org/10.3390/s16111926.
56. Daniyan, I.A.; Tlhabadira, I.; Daramola, O.O.; et al. Measurement and optimization of cutting forces during M200 TS milling process using the response surface methodology and dynamometer. *Procedia CIRP* **2020**, *88*, 288–293. https://doi.org/10.1016/j.procir.2020.05.050.
57. Wan, M.; Yuan, H.; Feng, J.; et al. Industry-oriented method for measuring the cutting forces based on the deflections of tool shank. *Int. J. Mech. Sci.* **2017**, *130*, 315–323. https://doi.org/10.1016/j.ijmecsci.2017.06.022.
58. Ducobu, F.; Mélice, E.; Rivière-Lorphèvre, E.; et al. Sensitivity Analysis of Various Geometries of PCD and Cemented Tungsten Carbide Cutting Tools during the Milling of GFRP Composite. *Polymers* **2022**, *14*, 1524. https://doi.org/10.3390/polym14081524.
59. Furukawa, Y.; Moronuki, N. Effect of Material Properties on Ultra Precise Cutting Processes. *CIRP Ann.* **1988**, *37*, 113–116. https://doi.org/10.1016/S0007-8506(07)61598-4.
60. Câmara, M.A.; Abrão, A.M.; Rubio, J.C.C.; et al. Determination of the critical undeformed chip thickness in micromilling by means of the acoustic emission signal. *Precis. Eng.* **2016**, *46*, 377–382. https://doi.org/10.1016/j.precisioneng.2016.06.007.
61. Medina-Clavijo, B.; Ortiz-de-Zarate, G.; Sela, A.; et al. In-SEM micro-machining reveals the origins of the size effect in the cutting energy. *Sci. Rep.* **2021**, *11*, 2088. https://doi.org/10.1038/s41598-021-81125-7.
62. Cui, Y.; Wang, D.; Zheng, M.; et al. Study on Cutting Performance and Wear Resistance of Biomimetic Micro-Textured Composite Cutting Tools. *Metals* **2025**, *15*, 697. https://doi.org/10.3390/met15070697.
63. Chang, X.; Gao, W.; An, J.; et al. Optical-grade diamond: Characteristics, synthesis, and recent research progress. *Funct. Diam.* **2025**, *5*, 2476690. https://doi.org/10.1080/26941112.2025.2476690.
64. Yuan, S.; Guo, X.; Huang, J.; et al. Sub-nanoscale polishing of single crystal diamond(100) and the chemical behavior of nanoparticles during the polishing process. *Diam. Relat. Mater.* **2019**, *100*, 107528. https://doi.org/10.1016/j.diamond.2019.107528.
65. Lv, Y.; Zhao, L.; Wang, X.; et al. Mitigating the Thermal Bottleneck in Polycrystalline Diamond Films by Gradient ICP Etching of the Nucleation Layer. *Materials* **2026**, *19*, 759. https://doi.org/10.3390/ma19040759.
66. Graebner, J.E. Thermal Conductivity of Diamond. In *Diamond: Electronic Properties and Applications*; Springer: Boston, MA, USA, 1995; pp. 285–318. https://doi.org/10.1007/978-1-4615-2257-7_7.
67. Zou, Z.; Zhang, T.; He, L. Multi-Objective Optimization of Tool Edge Geometry for Enhanced Cutting Performance in Turning Ti6Al4V. *Materials* **2025**, *18*, 4160. https://doi.org/10.3390/ma18174160.
68. Pimenov, D.Y.; da Silva, L.R.R.; Machado, A.R.; et al. A comprehensive review of machinability of difficult-to-machine alloys with advanced lubricating and cooling techniques. *Tribol. Int.* **2024**, *196*, 109677. https://doi.org/10.1016/j.triboint.2024.109677.
69. Hao, G.; Liu, Z.; Liang, X.; et al. Influences of TiAlN Coating on Cutting Temperature during Orthogonal Machining H13 Hardened Steel. *Coatings* **2019**, *9*, 355. https://doi.org/10.3390/coatings9060355.
70. Zhao, J.; Liu, Z.; Wang, B.; et al. Tool coating effects on cutting temperature during metal cutting processes: Comprehensive review and future research directions. *Mech. Syst. Signal Process.* **2021**, *150*, 107302. https://doi.org/10.1016/j.ymssp.2020.107302.
71. Baptista, A.; Silva, F.; Porteiro, J.; et al. Sputtering Physical Vapour Deposition (PVD) Coatings: A Critical Review on Process Improvement and Market Trend Demands. *Coatings* **2018**, *8*, 402. https://doi.org/10.3390/coatings8110402.
72. An, S.; Foest, R.D.; Fricke, K.; et al. Pretreatment of cutting tools by plasma electrolytic polishing (PEP) for enhanced adhesion of hard coatings. *Surf. Coat. Technol.* **2021**, *405*, 126504. https://doi.org/10.1016/j.surfcoat.2020.126504.
73. Lv, S.; Yang, M.; Jiang, M.; et al. Predictive thermal modeling for rough interfaces of Ti-6Al-4V chip and TiAlSiN-coated tool based on micro-contact analysis. *Int. J. Heat Mass Transf.* **2026**, *271 Pt 2*, 129361.
74. Li, Y.; Zhou, Z.; He, Y. Solid Lubrication System and Its Plasma Surface Engineering: A Review. *Lubricants* **2023**, *11*, 473. https://doi.org/10.3390/lubricants11110473.
75. Wu, X.; Jiang, Y.; Wu, T.; et al. Insight into the Mechanisms of Nitride Films with Excellent Hardness and Lubricating Performance: A Review. *Nanomaterials* **2023**, *13*, 2205. https://doi.org/10.3390/nano13152205.
76. Sousa, V.F.C.; Fernandes, F.; Silva, F.J.G.; et al. Wear Behavior Phenomena of TiN/TiAlN HiPIMS PVD-Coated Tools on Milling Inconel 718. *Metals* **2023**, *13*, 684. https://doi.org/10.3390/met13040684.
77. de Paiva, R.L.; da Silva, L.R.R.; Baldin, V.; et al. Review of innovative strategies and future prospects in challenging-to-machine materials. *Int. J. Adv. Manuf. Technol.* **2026**, *145*, 1667–1689. https://doi.org/10.1007/s00170-026-18428-4.

78. Feng, Y.; Zhang, L.; Ke, R.; et al. Thermal stability and oxidation behavior of AlTiN, AlCrN and AlCrSiWN coatings. *Int. J. Refract. Met. Hard Mater.* **2014**, *43*, 241–249. https://doi.org/10.1016/j.ijrmhm.2013.11.018.
79. Yan, C.; Yu, Y.; Mei, F.; et al. A Si-Nb co-alloyed AlCrN coating with good mechanical properties, excellent thermal stability and resistance to high temperature oxidation. *Surf. Coat. Technol.* **2024**, *484*, 130825. https://doi.org/10.1016/j.surfcoat.2024.130825.
80. Liu, J.; Mei, H.; Hua, J.; et al. High-Temperature Oxidation and Wear Resistance of TiAlSiN/AlCrN Multilayer Coatings Prepared by Multi-Arc Ion Plating. *Nanomaterials* **2025**, *15*, 503. https://doi.org/10.3390/nano15070503.
81. Mativenga, P.; Schoop, J.; Jawahir, I.S.; et al. Engineered design of cutting tool material, geometry, and coating for optimal performance and customized applications: A review. *CIRP J. Manuf. Sci. Technol.* **2024**, *52*, 212–228. https://doi.org/10.1016/j.cirpj.2024.06.001.
82. Pinto, G.; Silva, F.; Porteiro, J.; et al. Numerical Simulation Applied to PVD Reactors: An Overview. *Coatings* **2018**, *8*, 410. https://doi.org/10.3390/coatings8110410.
83. Baptista, A.; Silva, F.J.G.; Porteiro, J.; et al. On the Physical Vapour Deposition (PVD): Evolution of Magnetron Sputtering Processes for Industrial Applications. *Procedia Manuf.* **2018**, *17*, 746–757. https://doi.org/10.1016/j.promfg.2018.10.125.
84. Sun, F.; Zhu, A.; Liang, Z.; et al. Surface integrity of TC11 titanium alloy by electric pulse-assisted helical hole milling. *Tribol. Int.* **2025**, *204*, 110528. https://doi.org/10.1016/j.triboint.2025.110528.
85. Jackson, M.J.; Robinson, G.M.; Whitt, M.D.; et al. Achieving clean production with nanostructured coated milling tools dry machining low carbon steel. *J. Clean. Prod.* **2023**, *422*, 138523. https://doi.org/10.1016/j.jclepro.2023.138523.
86. Vereschaka, A.; Gurin, V.; Oganyan, M.; et al. Increase in tool life for end milling titanium alloys using tools with multilayer composite nanostructured modified coatings. *Procedia CIRP* **2019**, *81*, 1412–1416. https://doi.org/10.1016/j.procir.2019.04.173.
87. Devillez, A.; Schneider, F.; Dominiak, S.; et al. Cutting forces and wear in dry machining of Inconel 718 with coated carbide tools. *Wear* **2007**, *262*, 931–942. https://doi.org/10.1016/j.wear.2006.10.009.
88. Sebbe, N.; Fernandes, F.; Costa, R.; et al. Wear Behaviour and Machining Performance in Milling of INCONEL® 718 of TiAlVN and TiAlN/TiAlVN Coated Tools: A Comparative Study. In *Design, Simulation, Manufacturing: The Innovation Exchange*; Springer: Cham, Switzerland, 2024; pp. 319–330. https://doi.org/10.1007/978-3-031-61797-3_27.
89. Pedroso, A.F.V.; Sousa, V.F.; Sebbe, N.P.V.; et al. A Review of INCONEL® Alloy's Non-conventional Machining Processes. In *Flexible Automation and Intelligent Manufacturing: Establishing Bridges for More Sustainable Manufacturing Systems*; Silva, F.J.G., Pereira, A.B., Campilho, R.D.S.G., Eds.; Springer: Cham, Switzerland, 2024; pp. 773–783. https://doi.org/10.1007/978-3-031-38241-3_86.
90. Pawade, R.S.; Joshi, S.S.; Brahmankar, P.K.; et al. An investigation of cutting forces and surface damage in high-speed turning of Inconel 718. *J. Mater. Process. Technol.* **2007**, *192–193*, 139–146. https://doi.org/10.1016/j.jmatprotec.2007.04.049.
91. Zhang, S.; Li, J.F.; Wang, Y.W. Tool life and cutting forces in end milling Inconel 718 under dry and minimum quantity cooling lubrication cutting conditions. *J. Clean. Prod.* **2012**, *32*, 81–87. https://doi.org/10.1016/j.jclepro.2012.03.014.
92. Demirsöz, R.; Korkmaz, M.E.; Gupta, M.K. A novel use of hybrid Cryo-MQL system in improving the tribological characteristics of additively manufactured 316 stainless steel against 100 Cr6 alloy. *Tribol. Int.* **2022**, *173*, 107613. https://doi.org/10.1016/j.triboint.2022.107613.
93. Fang, N.; Wu, Q. A comparative study of the cutting forces in high speed machining of Ti–6Al–4V and Inconel 718 with a round cutting edge tool. *J. Mater. Process. Technol.* **2009**, *209*, 4385–4389. https://doi.org/10.1016/j.jmatprotec.2008.10.013.
94. Kónya, G.; Csorba, B.; Szabó, N.; et al. The Effects of Cutting Parameters on Cutting Force and Tribological Properties of Machined Surface Under Dry Turning of AISI304L Austenitic Stainless Steel. *J. Manuf. Mater. Process.* **2024**, *8*, 257. https://doi.org/10.3390/jmmp8060257.
95. Sebbe, N.P.V.; Fernandes, F.D.; Bernardi, H.H.; et al. Wear Behaviour and Machining Performance of PrimeCon Coating in Milling of Ti–6Al–4V. In *Design, Simulation, Manufacturing: The Innovation Exchange*; Springer: Cham, Switzerland, 2025; pp. 43–53. https://doi.org/10.1007/978-3-031-96413-8_5.
96. Lee, G.H.; Kim, B.; Jeon, J.B.; et al. Precipitate phase behavior and mechanical properties of Inconel 718 according to aging heat treatment time. *Mater. Sci. Eng. A* **2025**, *924*, 147776. https://doi.org/10.1016/j.msea.2024.147776.
97. Mašek, P.; Alagan, N.T.; Mára, V.; et al. Chip formation and morphology in cryogenic machining of Al-SiC composites. *Int. J. Adv. Manuf. Technol.* **2025**, *137*, 2899–2917. https://doi.org/10.1007/s00170-025-15337-w.
98. Mabrouki, T.; Courbon, C.D.; Zhang, Y.; et al. Some insights on the modelling of chip formation and its morphology during metal cutting operations. *Comptes Rendus Mécanique* **2016**, *344*, 335–354. https://doi.org/10.1016/j.crme.2016.02.003.
99. Guan, X.; Liu, D.; Qu, S.; et al. Multiple Deformation Mechanisms in Adiabatic Shear Bands of a Titanium Alloy during High Strain Rate Deformation. *Materials* **2024**, *17*, 3645. https://doi.org/10.3390/ma17153645.
100. Barry, J.; Byrne, G.; Lennon, D. Observations on chip formation and acoustic emission in machining Ti–6Al–4V alloy. *Int. J. Mach. Tools Manuf.* **2001**, *41*, 1055–1070. https://doi.org/10.1016/S0890-6955(00)00096-1.

101. Pérez-Salinas, C.; de Lacalle, L.N.L.; del Olmo, A.; et al. The relationship between the cutting-edge, tool wear, and chip formation during Inconel 718 dry cutting. *Int. J. Adv. Manuf. Technol.* **2024**, *132*, 6001–6017. https://doi.org/10.1007/s00170-024-13685-7.
102. Wang, R.; Yang, D.; Wang, W.; et al. Tool Wear in Nickel-Based Superalloy Machining: An Overview. *Processes* **2022**, *10*, 2380. https://doi.org/10.3390/pr10112380.
103. Korkmaz, M.E. Tribological performance and energy savings in sustainable machining of duplex stainless steel via hybrid Cryo-MQL. *Eur. Phys. J. Spec. Top.* **2026**. https://doi.org/10.1140/epjs/s11734-026-02144-x.
104. Musfirah, A.H.; Ghani, J.A.; Haron, C.H.C. Tool wear and surface integrity of inconel 718 in dry and cryogenic coolant at high cutting speed. *Wear* **2017**, *376–377*, 125–133. https://doi.org/10.1016/j.wear.2017.01.031.
105. Pereira, O.; Celaya, A.; Urbikaín, G.; et al. CO_2 cryogenic milling of Inconel 718: Cutting forces and tool wear. *J. Mater. Res. Technol.* **2020**, *9*, 8459–8468. https://doi.org/10.1016/j.jmrt.2020.05.118.
106. Ventura, C.E.H.; Hassui, A. Evaluation of static cutting forces and tool wear in HSM process applied to pocket milling. *Int. J. Adv. Manuf. Technol.* **2013**, *65*, 1681–1689. https://doi.org/10.1007/s00170-012-4290-1.
107. Anh, N.T.; Tung, T.T. Cutting force prediction in end milling processes: Analytical models and applications. *Appl. Eng. Sci.* **2025**, *23*, 100250. https://doi.org/10.1016/j.apples.2025.100250.
108. Balogun, V.A.; Mativenga, P.T. Impact of un-deformed chip thickness on specific energy in mechanical machining processes. *J. Clean. Prod.* **2014**, *69*, 260–268. https://doi.org/10.1016/j.jclepro.2014.01.036.
109. Wang, P.; Bai, Q.; Cheng, K.; et al. The Modelling and Analysis of Micro-Milling Forces for Fabricating Thin-Walled Micro-Parts Considering Machining Dynamics. *Machines* **2022**, *10*, 217. https://doi.org/10.3390/machines10030217.
110. Li, H.Z.; Liu, K.; Li, X.P. A new method for determining the undeformed chip thickness in milling. *J. Mater. Process. Technol.* **2001**, *113*, 378–384. https://doi.org/10.1016/S0924-0136(01)00586-6.
111. Sztankovics, I. Analytical and Experimental Study of the Start of the Chip Removal in Rotational Turning. *J. Exp. Theor. Anal.* **2024**, *2*, 103–120. https://doi.org/10.3390/jeta2040009.
112. Fulemová, J.; Sklenička, J.; Hnátík, J.; et al. Cutting Force Mechanisms in Drilling 90MnCrV8 Tool Steel: ANOVA and Theoretical Insights. *J. Manuf. Mater. Process.* **2026**, *10*, 38. https://doi.org/10.3390/jmmp10010038.
113. Nie, S.; Chen, L.; Yun, Z.; et al. An Experimental Study on the Thermomechanical Coupling Effects of Carbon-Fiber-Reinforced Polyetheretherketone under Dynamic Impact. *Polymers* **2024**, *16*, 2295. https://doi.org/10.3390/polym16162295.
114. Liu, H.; Zhang, J.; Jiang, Q.; et al. Material Removal Mechanisms in Ultra-High-Speed Machining. *Engineering* **2025**, *55*, 51–70. https://doi.org/10.1016/j.eng.2024.12.033.
115. Rao, C.J.; Sreeamulu, D.; Mathew, A.T. Analysis of Tool Life during Turning Operation by Determining Optimal Process Parameters. *Procedia Eng.* **2014**, *97*, 241–250. https://doi.org/10.1016/j.proeng.2014.12.247.
116. Sun, S.; Brandt, M.; Dargusch, M.S. Thermally enhanced machining of hard-to-machine materials—A review. *Int. J. Mach. Tools Manuf.* **2010**, *50*, 663–680. https://doi.org/10.1016/j.ijmachtools.2010.04.008.
117. Gao, C.; Zhang, L. Effect of cutting conditions on the serrated chip formation in high-speed cutting. *Mach. Sci. Technol.* **2013**, *17*, 26–40. https://doi.org/10.1080/10910344.2012.747887.